Korean J. Chem. Eng., **27**(2), 590-595 (2010)
DOI: 10.1007/s11814-010-0064-3

Equation of state for gaseous ethane determined from isotropic model potentials

Kenneth Monago†

Department of Pure and Industrial Chemistry, University of Port Harcourt,
P M B 5323 Choba, Port Harcourt, Nigeria
(*Received 24 February 2009 • accepted 1 June 2009*)

Abstract−A four-term virial equation of state was combined with isotropic model potentials to predict accurate volumetric and caloric thermodynamic properties of ethane in the gas phase. The parameters of the model potentials were determined from a fit to speed-of-sound data alone; no other data were used. The approximation used for the fourth virial coefficient included all interactions that contain up to two triplet potentials. Predicted ordinary second and third virial coefficients are in agreement with the data of Funke et al. [8]; we believe that predicted fourth virial coefficients are reliable and accurate. In the subcritical temperature region, the equation of state predicted compressibility factors that deviate by less than 0.04 percent at densities of up to 2.7 mol/dm^3 ($\approx 0.4\rho_c$). At supercritical temperatures, compressibility factors deviate by less than 0.02 percent at densities of up to 2.6 mol/dm^3; also, in this region predicted isobaric heat capacity agrees with available data to within uncertainties of 0.4 percent at densities above 3 mol/dm^3. We demonstrated that the four-term virial equation is more accurate than the three-term analogue.

Key words: Equation of State, Ethane, Model Potential Functions, Ordinary Fourth Virial Coefficient, Acoustic Fourth Virial Coefficient, Sotropic Model Potentials, Speed of Sound

INTRODUCTION

Accurate knowledge of volumetric and caloric thermodynamic properties is required in custody-transfer metering of natural gas. In the gas phase, the required information is preferably correlated with a virial equation of state truncated after the third term [1,2]. The reasons for truncating after the third coefficient are probably the computational effort required for extension to the fourth term and the mistaken belief that inclusion of the fourth virial coefficient is unproductive [3].

Our primary goal is to develop a virial equation of state for natural gas systems, which by truncating the expansion after the fourth term, will offer superior performance to what is currently available, particularly within the so-called custody-transfer region: T/[K]= 300±30 and P/[MPa]≤12. As a major component of natural gas, accurate virial coefficients of ethane are a necessary first-step for developing reliable models for the mixture. Furthermore, it appears that little or no reliable values exist for the virial coefficients of ethane at temperatures below 200 K [4]; consequently, this paper will attempt to fill this gap in our knowledge of the properties of this technically important substance.

In previous work, we have applied the virial equation of state truncated after the fourth virial coefficient to argon [5] and methane [6].

From a statistical mechanical point of view, ethane is a non-rigid linear molecule; consequently, the true interaction potentials of the molecule significantly differ in several respects from the isotropic model employed in this work. Nevertheless, it is hoped that due to rapid rotation of the molecule, effective isotropic potential parameters will be derived from a fit to selected thermodynamic properties data, and that the resulting parameters will permit some extrapolation in temperature and density.

In this paper, the model potential parameters are fitted to the acoustic data of Estrada-Alexanders [7] alone, and the parameters will be tested with the experimental volumetric and caloric properties [4,7-9].

†To whom correspondence should be addressed.
E-mail: kmonago@yahoo.com

THEORY

If we start from the definitional equation

$$w^2 = -\frac{v^2}{M}\left(\frac{\partial P}{\partial v}\right)_S, \tag{1}$$

the virial equation of state may be related to the equilibrium speed of sound in the following six steps:

$$Z = 1 + B/V + C/V^2 + D/V^3 \tag{2}$$

$$V = ZRT/P, \tag{3}$$

$$-\frac{V^2}{RT}\left(\frac{\partial P}{\partial V}\right)_T = \frac{1}{\beta_r}, \tag{4}$$

$$\frac{1}{\beta_r} = 1 + 2B/V + 3C/V^2 + 4D/V^3, \tag{5}$$

$$C_v = C_v^{pg} - (R/V^3)[(2TB' + T^2B'')V^2 + (2TC' + T^2C'')V/2 + (2TD' + T^2D'')/3], \tag{6}$$

$$(\partial P/\partial T)_v = R[V^3 + (B + TB')V^2 + (C + TC')V + (D + TD')]/V^4 \tag{7}$$

$$C_p = C_v + \frac{V^2\beta_r(\partial P/\partial T)_v^2}{R}; \tag{8}$$

Finally,

$$w^2=RTC_p/M\beta_r C_v \quad (9)$$

In the above equations, Z is the compressibility factor, V is the molar volume, C_v and C_p are, respectively, the isochoric and isobaric heat capacity, C_v^{pg} is C_v for the hypothetical ideal gas, M is the molar mass of the gas, S is entropy and w is the sound speed. The functions B, C and D are, respectively, ordinary second, third and fourth virial coefficients, and these are related by theory to pair- and triplet-intermolecular potential functions by integral expressions; in the language of linear graph [6,10],

$-2B=$ ——— (10)

$-3D=$ 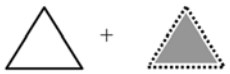 (11)

$-8D=3$ 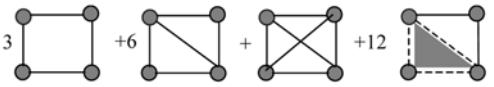 (12)

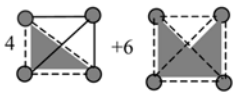

In the scheme above, an unbroken line represents the two-body Mayer function, a dashed line represents a Boltzmann factor, and a shaded triangular plate represents the three-body Mayer function. Explicit integral expressions for individual graphs and relevant definitions have been given elsewhere [5,6]. In Eq. (6) B″, C″ and D′ are, respectively, the first temperature derivatives of the virial coefficients B, C and D; B″, C″ and D′ are the corresponding second temperature derivatives.

In Eq. (2) the expansion of pressure in powers of density assumes that the total intermolecular potential energy $\phi(\mathbf{r}^N)$ is the sum of pair and triplet interactions:

$$\phi(\mathbf{r}^N)=\sum_{i=1}^{N-1}\sum_{j=i+1}^{N}\phi_{ij}+\sum_{i=1}^{N-2}\sum_{j=i+1}^{N-1}\sum_{k=j+1}^{N}\Delta\phi_{ijk} \quad (13)$$

where, ϕ_{ij} is the pair-potential energy and $\Delta\phi_{ijk}$ is the non-additive three-body potential energy of interaction. However, whereas Eqs. (10) and (11) are exact, Eq. (12) is exact only at the level of graphs with no more than two triplet potentials; graphs with higher triplet potentials and the non-additive four-body potential have been neglected.

A convenient model pair potential function is that proposed by Maitland and Smith [11]:

$$\phi(r_{ij})=\frac{6\varepsilon}{n-6}\{(r_m/r)^n-(n/6)(r_m/r)^6\}; \quad (14)$$

It has four parameters--ε, the numerical value of the potential at its minimum; r_m, the radial distance at which $\phi=-\varepsilon$ and two shape parameters m and κ--which determine the repulsive exponent according to the linear equation

$$n=m+\kappa\{(r/r_m)-1\} \quad (15)$$

Non-additive three-body forces are modeled by the Axilrod-Teller triple dipole energy; hence,

$$\Delta\phi_{123}=\nu_{123}(1+3\cos\theta_1\cos\theta_2\cos\theta_3)/(r_{12}r_{13}r_{23})^3 \quad (16)$$

Eq. (16) adds the fifth parameter to the model, namely, ν_{123}, the three-body strength coefficient.

Translational quantum corrections were applied to all the virial coefficients [12] as standard implementation of our virial equation of state; however, no attempt was made to ascertain the significance of these corrections for ethane.

NUMERICAL METHODS

Parameters in the model potential functions were determined by solving the nonlinear least square problem

$$\chi^2=\mathbf{R}^T\mathbf{R} \quad (17)$$

where,

$$R_i(\mathbf{x})=(w_{i,cal}-w_{i,expt})/s_i\sqrt{N-N_p} \quad (18)$$

Here, $\mathbf{x}$ is the parameter vector, $w_{i,expt}$ is the i-th experimental speed of sound value, $w_{i,cal}$ is the calculated value for the speed of sound at the i-th data point, N is the total number of acoustic data points, N_p is the number of adjustable parameters in the model and s_i is the estimated standard deviation of $w_{i,expt}$.

Each w_{cal} (T_i, P_i) was calculated in the following way. First, the virial coefficients B, C and D together with their first two temperature derivatives were calculated along 12 experimental isotherms from the integral expressions that relate them to $\phi(r_{ij})$ and $\Delta\phi_{123}$. Next, at each experimental temperature and pressure of the data points, we determined Z from

$$Z^4-Z^3-(BP/RT)Z^2-C(P/RT)^2Z-D(P/RT)^3=0 \quad (19)$$

Thereafter, V was calculated from Eq. (3), followed by C_v and C_p, respectively, from Eqs. (6) and (8). Finally, w_{cal} (T_i, P_i) was calculated from Eq. (9).

Values of C_v^{pg} required in Eq. (6) were obtained from those determined by Estrada-Alexanders [7] from his acoustic data. In Eq. (9), the values we used for the molar mass of ethane and the molar gas constant were, respectively, M=0.0300696 kg mol^{-1} and for R= 8.314472 J mol^{-1} K^{-1}.

The dimensionless statistic, χ^2, was minimized as described elsewhere [6]. The virial coefficients and their temperature derivatives were calculated as described in refs. 5 and 6.

THE FIT TO THE SPEED OF SOUND

The experimental speed-of-sound data of Estrada-Alexanders [7] are given on 17 isotherms in the region $0.72\le T/T_c\le 1.47$ and $\rho\le\rho_c/2$; however, acoustic data from the following 12 out of the 17 experimental isotherms were actually employed in the parameter fitting: 220 K, 235 K, 250 K, 265 K, 275 K, 285 K, 295 K, 305 K, 315 K, 330 K, 340 K and 365 K. On each of the above 12 isotherms, we limited acoustic data employed in the fit to those at densities that were no higher than 1. 03 mol dm^{-3} and each datum was assigned an uncertainty of 0.003 percent. During the optimization, it appeared that the parameter space contained many local minima, perhaps corresponding to different temperature averages of the true anisotropic potential of interaction. The following set of parameters that minimized Eq. (17) and best reproduced the volumetric data of Funke et al. [4,8], was considered the most useful set:

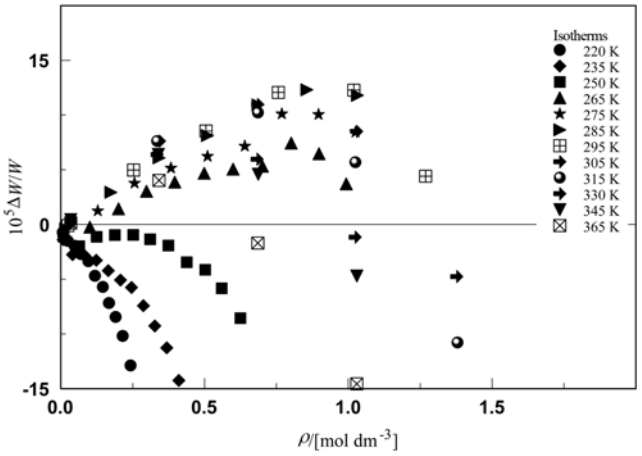

Fig. 1. Fractional errors $\Delta W/W_{expt}$ in experimental [7] speed-of-sound of ethane from the fit. $\Delta W = W_{expt} - W_{cal}$.

$$\left.\begin{aligned} r_m &= 0.450497 \text{ nm} \\ \varepsilon/k &= 393.3354 \text{ K} \\ m &= 32.510 \\ \kappa &= 12.604 \\ \nu_{123}/k &= 0.013901 \text{ K nm}^9 \end{aligned}\right\} \quad (20)$$

The deviations of the experimental speeds of sound from those given by the final model are displayed in Fig. 1.

THE VIRIAL COEFFICIENTS OF ETHANE

Fig. 2 shows deviations in experimental ordinary [8,9] and acoustic [7] second virial coefficients of ethane from those predicted by the present isotropic model. Since the acoustic virial coefficients themselves had been determined from the speed-of-sound data employed in this work, the parameters of Eq. (20) are indirectly fitted to these virials. Nevertheless, some systematic deviations are apparently present, especially below a temperature of about 250 K and

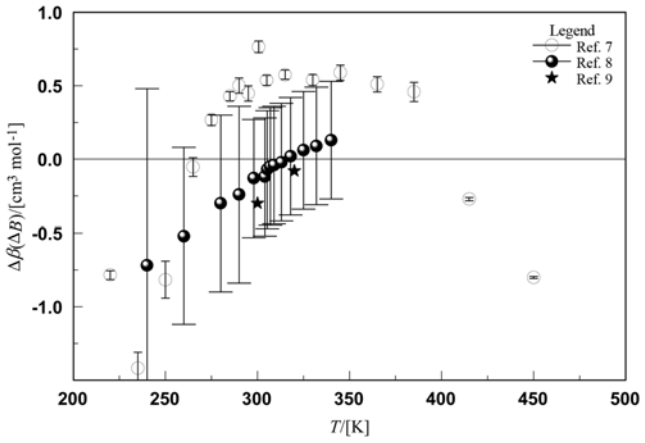

Fig. 2. Deviations in experimental ordinary [8,9] and acoustic [7] second virial coefficients of ethane with respect to values predicted from Eq. (20). $\Delta\beta = \beta_{expt} - \beta_{cal}$. Open symbols, acoustic virial coefficients; filled symbols, ordinary virial coefficients.

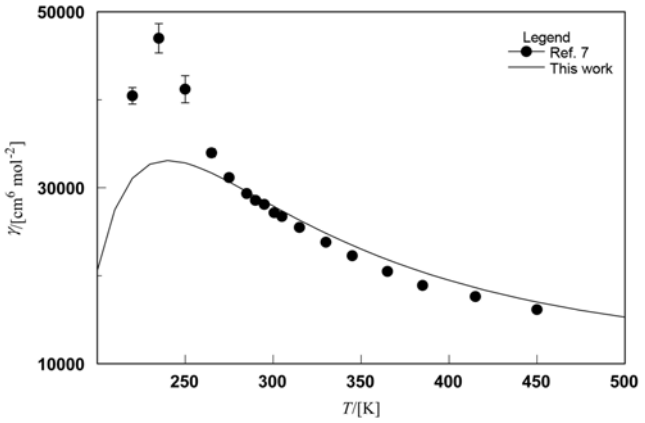

Fig. 3. Experimental [7] and predicted acoustic third virial coefficients of ethane with respect to values predicted from Eq. (20).

again above 425 K. However, to what extent those deviations reflect shortcomings in the model rather than error in the data is uncertain. Fig. 2 also compares ordinary, second virial coefficients of ethane predicted by the present equation of state with the experimental data of refs. 8 and 9. Although the deviations clearly appear systematic, nevertheless, the agreement obtained here may be compared with those obtained with the acoustic analogue (±0.5 cm^3/mol, compared with ±1 cm^3/mol).

Acoustic third virial coefficients predicted by the model are compared with the data of ref. 7 in Fig. 3. We see that there is only fair agreement ($\Delta\gamma$=±1,000 cm^6/mol^2) above a temperature of about 275 K; conversely, below this temperature, acoustic third virial coefficients predicted by the equation of state may be too low by as much as 14,000 cm^6/mol^2. Estrada-Alexanders [7] himself compared his acoustic third virial coefficients with the data of other workers and concluded that fair agreement existed only above 273 K. It would appear, therefore, that new experimental acoustic third virial coefficients of ethane, particularly below about 275 K, are required in order to resolve the data uncertainty. In the same vein, Fig. 4 shows that predicted ordinary third virial coefficients are in much better agreement with experimental values than the situation in Fig. 3. Fig.

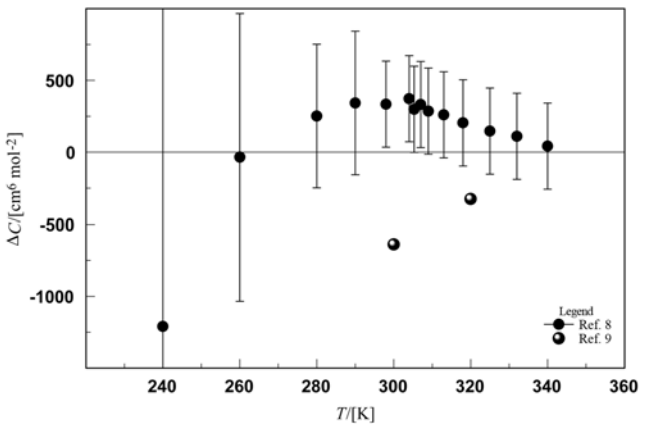

Fig. 4. Deviations of experimental [8,9] ordinary third virial coefficients of ethane with respect to values predicted from Eq. (20).

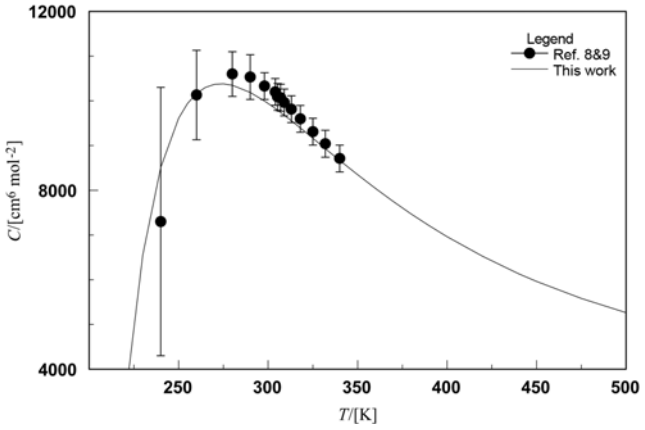

Fig. 5. Experimental and predicted ordinary third virial coefficient of ethane as a function of temperature.

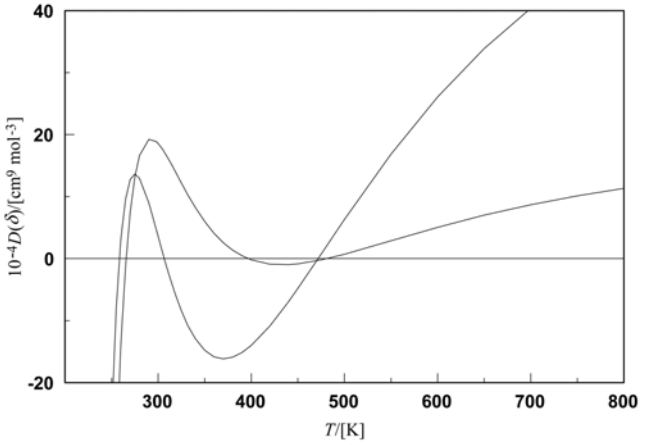

Fig. 6. Ordinary and acoustic fourth virial coefficient of ethane predicted from potential parameters Eq. (20). Solid line, ordinary virial coefficient; dotted line, acoustic virial coefficient.

5 shows ordinary third virial coefficients of ethane as a function of temperature. In Fig. 6 we show ordinary and acoustic fourth virial coefficients as functions of temperature. We see that not only does the ordinary fourth virial coefficient of ethane possess two turning points, which is contrary to the behavior of this function in simpler gases including methane, D is negative at the minimum. Similar comments can be made for the acoustic fourth virial coefficient of ethane.

It would appear that few reliable tabulations of the virial coefficients of ethane below 200 K exist [4]; in Table 1 we have, therefore, tabulated values of B, C and D predicted by our equation of state in the temperature range 95-550 K.

PROPERTIES OF THE SATURATED VAPOUR

Fig. 7 compares vapor density at saturation predicted by our method with the experimental data of Funke et al. [4]; these data consist

Table 1. The virial coefficients of ethane

T [K]	B [cm^3 mol^{-1}]	C×10^{-3} [cm^6 mol^{-2}]	D×10^{-6} [cm^9 mol^{-3}]	T [K]	B [cm^3 mol^{-1}]	C×10^{-3} [cm^6 mol^{-2}]	D×10^{-6} [cm^9 mol^{-3}]
95	−2694.9	−20699	−1040550	240	−287.15	8.5100	−1.4476
100	−2283.4	−12185	−419543	260	−244.37	10.165	−0.13944
105	−1965.0	−7490.1	−183597	270	−226.39	10.368	0.07500
110	−1713.4	−4776.0	−86142	280	−210.24	10.348	0.16629
115	−1510.9	−3141.5	−42900	290	−195.65	10.188	0.19247
120	−1345.3	−2121.7	−22490	300	−182.40	9.9415	0.18566
125	−1207.9	−1465.4	−12326	305.32	−175.85	9.7887	0.17507
130	−1092.5	−1031.7	−7020.8	309	−171.49	9.6771	0.16618
135	−994.48	−738.08	−4136.2	313	−166.92	9.5518	0.15562
140	−910.38	−535.17	−2509.8	318	−161.42	9.3909	0.14169
145	−837.58	−392.33	−1562.9	320	−159.28	9.3257	0.13602
150	−774.05	−290.12	−995.679	332	−147.21	8.9301	0.10264
155	−718.20	−215.92	−647.200	340	−139.79	8.6679	0.08221
160	−668.78	−161.35	−428.188	350	−131.14	8.3476	0.05971
165	−624.77	−120.77	−287.723	360	−123.13	8.0395	0.04085
170	−585.37	−90.286	−195.982	370	−115.68	7.7460	0.02558
175	−549.91	−67.181	−135.080	380	−108.74	7.4683	0.01360
180	−517.86	−49.535	−94.055	390	−102.25	7.2070	0.00454
185	−488.75	−35.969	−66.056	400	−96.184	6.9619	−0.00198
190	−462.21	−25.481	−46.724	420	−85.139	6.5187	−0.00887
195	−437.93	−17.336	−33.236	440	−75.350	6.1336	−0.00970
200	−415.64	−10.988	−23.739	450	−70.862	5.9608	−0.00847
210	−376.13	−2.1456	−12.183	475	−60.659	5.5797	−0.00219
220	−342.23	3.2682	−6.2223	500	−51.700	5.2618	0.00700
230	−312.85	6.5579	−3.0969	550	−36.711	4.7744	0.02872

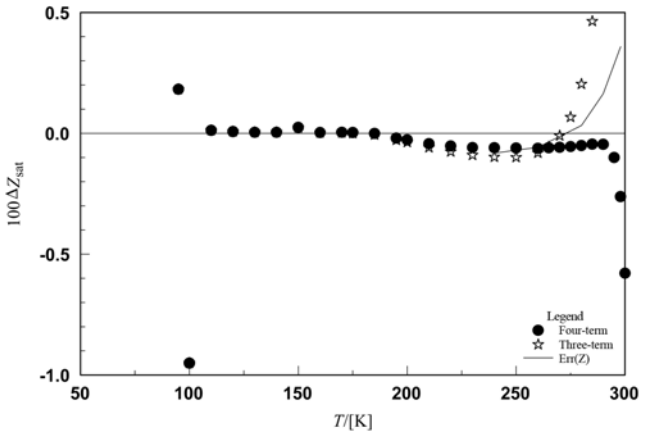

Fig. 7. Deviations of compressibility factors of the saturated vapor of ethane with respect to the data of Funke et al [4]. The four-term and three-term equations were implemented with the same set of potential parameters. The solid line is the function $\Delta Z_{sat}=\Delta B\rho+\Delta C\rho^2$; where, ΔB, ΔC are discrepancies.

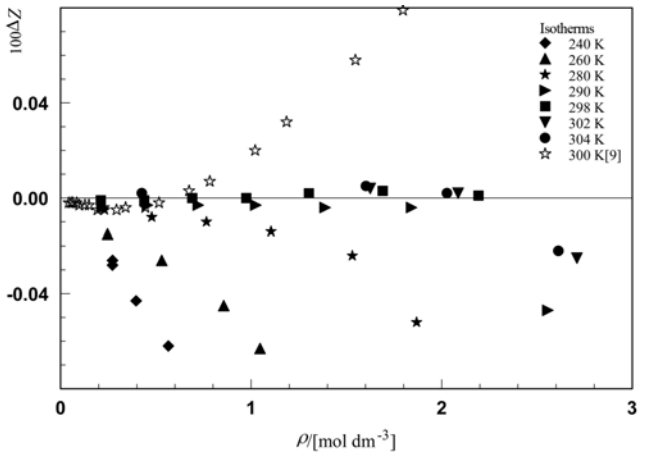

Fig. 8. Deviations of compressibility factors of ethane predicted by Eq. (20) from experimental values in the temperature range 240-304 K. The 300 K isotherm is based on ref. 9, all others are based on ref. 8.

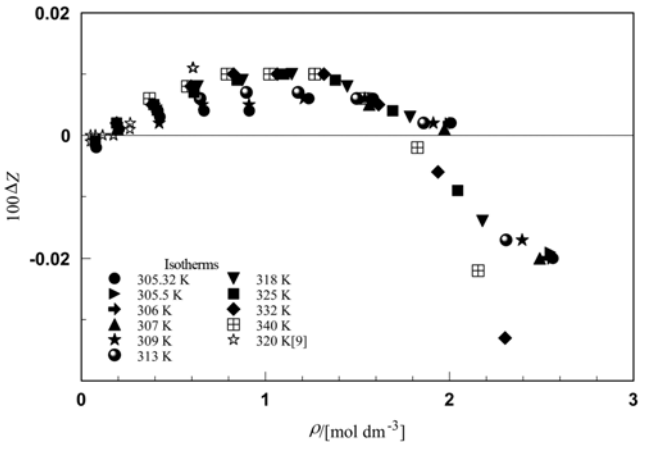

Fig. 9. Deviations of compressibility factors of ethane predicted by Eq. (20) from experimental values in the temperature range 305-340 K. The 320 K isotherm is based on ref. 9, all others are based on ref. 8.

of two sections. In the temperature range, T/[K]≤175, the 'experimental' saturated density was calculated from a virial equation of state truncated after the second term and based on an isotropic potential model; at higher temperatures the saturated density was determined experimentally. At the two lowest temperatures, Z_{sat} of ref. 4 differ from our results by nearly 1 percent. Furthermore, because in the limit of zero density all gases become perfect in their P-ρ-T behavior, we believe that the values of Z_{sat} given in ref. 4 for T/[K]≤ 100 are in error.

Fig. 7 shows that our results agree quite well ($\Delta Z_{sat}\leq -0.00043$) with the data of ref. 4 up to a temperature of about 210 K; the agreement is only fair ($\Delta Z_{sat}\leq -0.00062$) in the range 220≤T/[K]≤280. Again, quite good agreement ($\Delta Z_{sat}\leq -0.00046$) exists between 285-290 K; above 290 K, the equation of state breaks down because the value of the vapor density is greater than the accuracy of the model. The solid curve in Fig. 7 represents the function ($\rho\Delta B+\rho^2\Delta C$); where, ΔB and ΔC are, respectively, the discrepancies in experimental and predicted second and third virial coefficients. It is clear that the apparent error in Z_{sat} can be explained in terms of these discrepancies and not the virial equation of state itself. The errors in the virial coefficients could have come about because the potential parameters are temperature-average values and (or) the acoustic data from which the parameters were derived may not have been as accurate as for argon [5] and methane [6].

Fig. 7 also shows that the four-term virial equation of state is significantly more useful than the three-term analogue if both are implemented with the same set of potential parameters.

COMPARISON WITH OTHER EXPERIMENTAL DATA

In Figs. 8 and 9 we compare compressibility factors predicted from the present equation of state with experimental P-ρ-T data [8,9]. The apparent systematic deviations observed in Fig. 8 on the 240 K and 260 K isotherms can be explained in terms of the probable error, ΔZ; where, $\Delta Z=\rho\Delta B+\rho^2\Delta C$. However, since the mutual disagreement in predicted and experimental virial coefficients is well within the quoted experimental uncertainties, the question as to whether or not the model failed at these temperatures remains unanswered. Above 280 K and up to 304 K, values of compressibility factor predicted by our model agree with the experimental data of Funke et al. [8] to within 0.04 percent up to 2.7 mol/dm^3 in density, as Fig. 8 shows. In contrast, the data of Hou et al. [9] on the 300 K isotherm deviate in a systematic manner, reaching 0.06 percent at just 1.547 mol/dm^3, as Fig. 8 also shows. Fig. 9 shows that in the higher temperature range 305-340 K, our predicted values agree with the data of Funke et al. to within 0.02 percent up to 2.6 mol/dm^3 in density.

It is a widely held view that the virial expansion is best truncated after the third-term; consequently, little tabulation of the fourth virial coefficients exists. We have argued that this is misconceived and that accurate fourth virial coefficients can extend the density over which the viral expansion is capable of very high accuracy. We have

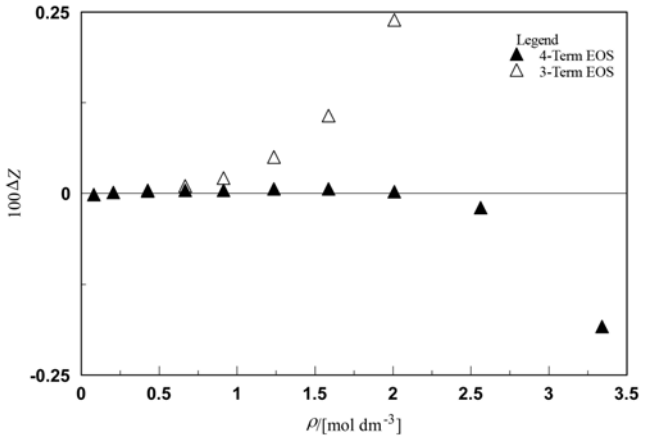

Fig. 10. Deviations in the compressibility factors of ethane along the critical isotherm (305.322 K) predicted by three-term and four-term virial equations of state. The experimental values are those of ref. 8.

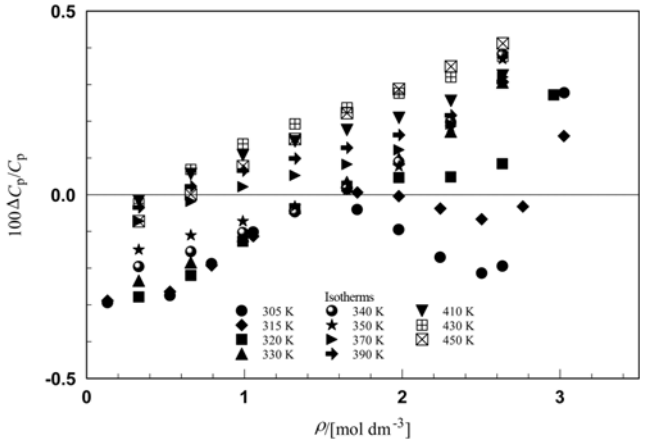

Fig. 11. Fractional errors in heat capacity of ethane predicted from Eq. (20) with respect to the data of Estrada-Alexanders [7] in the temperature range 305-450 K.

compared the performances of three-term and four-term procedures in Fig. 7. In Fig. 10, we further show the performances of the two equations of state along the critical isotherm (305.322 K). Detailed consideration of these results shows that whereas the three-term equation is accurate to better than 0.05 percent at 1.25 mol/dm^3, the four-term analogue is accurate to better than 0.02 percent at 2.6 mol/dm^3. However, we should point out that the above result is so, in part at least, because the parameters of Eq. (20) were fitted to the four-term implementation and that slightly different results might have been obtained had parameters fitted to the three-term version been used in the latter equation of state.

Fig. 11 compares values of isobaric heat capacity predicted by the present equation of state with the data of Estrada-Alexanders [7]. The latter are not experimental values, but were calculated from experimental speed-of-sound values by a direct integration method. Some of these data were tabulated along isotherms different from experimental temperatures; consequently, ideal-gas heat capacity required as initial condition was obtained from an equation reported in ref. 7, which was based on the spectroscopic data of Chao et al. [14]. Ref. 7 does not provide estimates of uncertainties in the heat capacity; however, the ideal-gas heat capacity determined by extrapolation of his acoustic data showed fractional errors of up to 0.0025, when compared with the data of ref. 14. Fig. 11 shows that in the super-critical temperature region, the mutual disagreement between our predicted values and the data of ref. 7 remain within ±0.4 percent at densities, $\rho_n \leq 3$ mol/dm^3.

CONCLUSIONS

The results presented in this paper demonstrate that a virial equation of state based on isotropic potential models can predict ordinary virial coefficients of ethane essentially to within the experimental uncertainties of the best available volumetric data. The inability of the model to predict acoustic virial coefficients of ethane over the same temperatures raises question as to the consistency of available experimental acoustic and ordinary virial coefficients of ethane. In the subcritical temperature states, the resulting four-term virial equation of state predicted compressibility factors for ethane to within 0.04 percent at densities up to 2.7 mol/dm^3 (or $\approx 0.4\rho_c$). In the supercritical temperature region, compressibility factors were predicted to within 0.02 percent up to 2.6 mol/dm^3 in density. Further, in the supercritical temperature region, predicted isobaric heat capacity, when compared with available data, is accurate to within fractional errors no worse than 0.4 percent and up to 3.3 mol/dm^3 in density.

REFERENCES

1. J. F. Estela-Uribe, J. Jeramillo, M. A. Salazar, J. P. M. Trusler, *Fluid Phase Equilibria*, **204**(2), 169 (2003).
2. M. Jaeschke, S. Andibert, P. Caneghem, A. E. Humphreys, R. Jansen-van Resmalem, Q. Pellei, J. P. J. Michels and J. A. Schonten, *SPE Prod. Engng*., Aug., 350 (1991).
3. J. P. M. Trusler, *Int. J. Thermophys*., **18**, 635 (1997).
4. M. Funke, R. Kleinrahm and W. Wagner, *J. Chem. Thermodyn*., **34**, 2017 (2002).
5. K. O. Monago, *Chem. Phys*., **316**, 9 (2005).
6. K. O. Monago, *Chem. Phys*., **337**, 125 (2007).
7. A. F. Estrada-Alexanders, PhD thesis, University of London (1996).
8. M. Funke, R. Kleinrahm and W. Wagner, *J. Chem. Thermodyn*., **34**, 2001 (2002).
9. H. Hou, J. C. Holste, K. R. Hall, K. N. Marsh and B. E. Gammon, *J. Chem. Eng. Data*, **41**, 344 (1996).
10. H. L. Fiedman, *Ionic theory based on cluster expansion*, Wiley Interscience, 36 (1962).
11. G. C. Maitland and E. B. Smith, *Chem. Phys. Lett*., **22**, 443 (1973).
12. K. O. Monago, *Chem. Phys. Lett*., **430**, 21 (2006).
13. K. Lucas, *Int. J. Thermophys*., **7**, 477 (1986).
14. J. Chao, R. C. Wilhoit and B. J. Zwolinski, *J. Phys. Chem. Ref. Data*, **2**, 427 (1973).